

# A near zero coefficient of thermal expansion ceramic: Tantalum oxyfluoride

Stephanie Sawhill, Ender Savrun\*

Sienna Technologies, Inc., 19501 144th Ave. NE Suite F-500, Woodinville, WA 98072, United States

Received 31 May 2011; received in revised form 10 October 2011; accepted 12 October 2011

Available online 25 October 2011

## Abstract

Cubic tantalum oxyfluoride ( $\text{TaO}_2\text{F}$ ) powders were synthesized and consolidated by hot pressing. The effects of sodium fluoride ( $\text{NaF}$ ) and lithium fluoride ( $\text{LiF}$ ) sintering aids on the densification and microstructure of  $\text{TaO}_2\text{F}$  were investigated. Hot pressing conditions employed in this study appeared to change the stoichiometry of  $\text{TaO}_2\text{F}$ , and most likely created an oxygen deficient  $\text{TaO}_{2-\delta}\text{F}$ . It was shown that  $\text{TaO}_2\text{F}$  decomposes in air at temperatures  $\geq 500^\circ\text{C}$  but that the kinetics of its decomposition is very slow up to  $750\text{--}800^\circ\text{C}$ . Hot-pressed  $\text{TaO}_2\text{F}$  had a near-zero coefficient of thermal expansion over  $25\text{--}600^\circ\text{C}$  that did not change after exposure to air for extended periods of time (24 h) at  $600^\circ\text{C}$ .  $\text{TaO}_2\text{F}$  has no inherent absorption bands in the mid-infrared (mid-IR) region up to about  $5\text{ }\mu\text{m}$  suggesting that polycrystalline  $\text{TaO}_2\text{F}$  ceramic can be IR transparent provided that it can be densified without altering its chemistry.

© 2011 Elsevier Ltd and Techna Group S.r.l. All rights reserved.

**Keywords:** A. Hot-pressing; C. Optical properties; C. Thermal expansion; Tantalum oxyfluoride

## 1. Introduction

Infrared transparent materials with low thermal expansion and high thermal shock resistance that can operate at high temperatures are required in many industrial applications. Crystalline oxides with low thermal expansion are nearly always anisotropic materials where optical properties are strongly influenced by grain size and grain boundary scattering. Their thermal expansions, usually a mixture of positive and negative values, vary with directions. This thermal expansion anisotropy causes microcracking upon thermal cycling. Cubic materials are isotropic. They do not suffer from the optical transparency loss by grain boundary scattering, and do not show thermal expansion anisotropy thus are immune to the microcracking.

Recently, Sleight and his group at Oregon State University [1] demonstrated that cubic  $\text{TaO}_2\text{F}$  powders have exceptionally low thermal expansion ( $0.1\text{--}0.3 \times 10^{-6}^\circ\text{C}^{-1}$ ) over the temperature range  $-250^\circ\text{C}$  to  $525^\circ\text{C}$ . Since  $\text{TaO}_2\text{F}$  is cubic, grain size and grain boundaries should not cause loss of optical or IR transparency, therefore, polycrystalline  $\text{TaO}_2\text{F}$  can potentially offer high thermal shock resistance and infrared transparency in mid-IR region.

In a phase pure, cubic polycrystalline ceramic, such as  $\text{TaO}_2\text{F}$ , the optical transmission is governed by the scattering of the light by the residual porosity. Even a very low residual porosity of 0.1% can completely deteriorate the transparency in an optical ceramic [2]. Therefore, to achieve optical transparency in polycrystalline  $\text{TaO}_2\text{F}$  either the porosity must be totally eliminated or a monomodal pore size distribution with pore size much less than wavelength of electromagnetic radiation must be achieved to eliminate scattering. However,  $\text{TaO}_2\text{F}$  has not been densified; therefore, the properties of dense polycrystalline  $\text{TaO}_2\text{F}$  are not known.

In this study,  $\text{TaO}_2\text{F}$  powders were synthesized and densified by hot pressing with and without use of a sintering aid sodium fluoride,  $\text{NaF}$ . Coefficients of thermal expansions and in-line IR transmissions of polycrystalline  $\text{TaO}_2\text{F}$  ceramics were measured. The thermochemical stability of  $\text{TaO}_2\text{F}$  ceramic was evaluated in air and argon environments. To our knowledge, this was the first time polycrystalline  $\text{TaO}_2\text{F}$  was produced and its thermal coefficient of expansion, IR transmission, and thermochemical stability in air were investigated.

## 2. Experimental

High purity  $\text{TaO}_2\text{F}$  powders are not commercially available and were therefore synthesized using a procedure developed by

\* Corresponding author. Tel.: +1 425 485 7272; fax: +1 425 485 8651.

E-mail addresses: [ender.savrun@siennatech.com](mailto:ender.savrun@siennatech.com), [e.savrun@clearwire.net](mailto:e.savrun@clearwire.net) (E. Savrun).

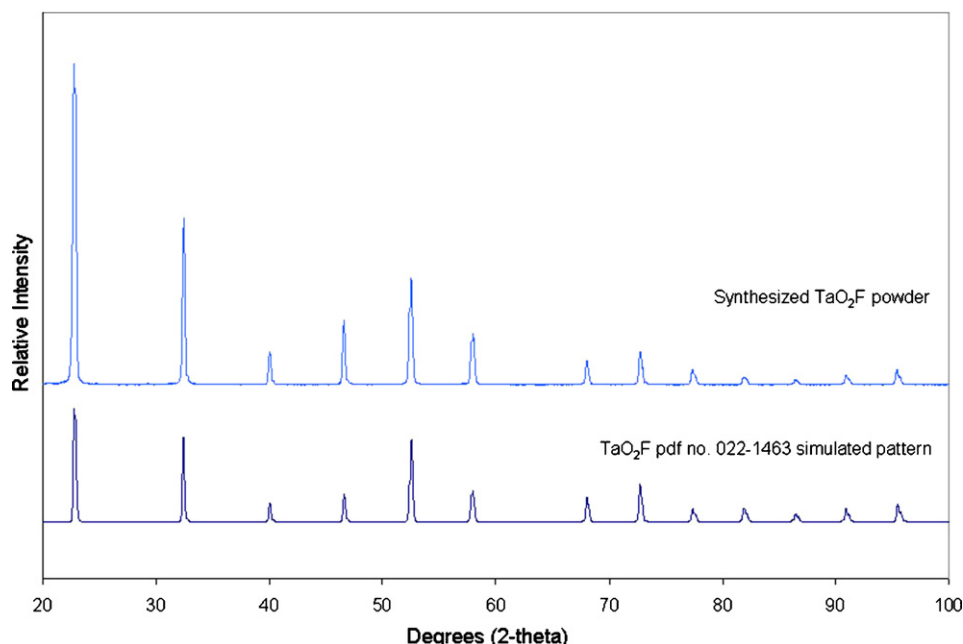


Fig. 1. XRD pattern for synthesized  $\text{TaO}_2\text{F}$  powder with simulated JCPDS PDF for  $\text{TaO}_2\text{F}$  (No. 022-1463).

Tao and Sleight [1]. Ta powder was dissolved in HF (48%) in a Teflon beaker at 80 °C, dried and calcined at 300 °C in air for 6 h. The  $\text{TaO}_2\text{F}$  powder was white in color.

$\text{TaO}_2\text{F}$  powders were ball-milled in acetone with high purity zirconia (99.9%) grinding media using an acrylate based dispersant for 4–24 h prior to hot pressing. In some cases, up to 1% NaF as a sintering aid was added to help densification during hot-pressing. Hot pressing was carried out in a graphite die at temperatures in the range of 700–1500 °C and pressures in the range of 46–100 MPa in argon atmosphere.

Thermal gravimetric analysis (TGA) and differential thermal analysis (DTA) of  $\text{TaO}_2\text{F}$  powders, as-prepared and after ball-milling, were carried out in air and argon (Ar) environments using a Netzsch instrument model STA 409 simultaneous TGA/DTA with mass spectrometer for evolved gases. TGA/DTA analyses were carried out from room temperature up to 1200 °C using a ramp rate of 5 °C/min. X-ray diffraction (XRD) measurements were carried out using the pressed powder technique on a Siemens D5000 Diffractometer with a  $\text{Cu K}\alpha$   $\lambda = 1.5418$  Å radiation source using a scan range of 20° (2-theta) up to 130° (2-theta). XRD samples were prepared by crushing  $\text{TaO}_2\text{F}$  powder or hot-pressed  $\text{TaO}_2\text{F}$  samples into fine powders. In-line IR transmission data and IR spectra were obtained using a Nicolet Nexus 670 IR spectrometer. IR spectra for  $\text{TaO}_2\text{F}$  powders and crushed  $\text{TaO}_2\text{F}$  hot-pressed samples were acquired using the KBr pellet method. IR transmission spectra of polycrystalline  $\text{TaO}_2\text{F}$  were acquired using polished 1 cm × 1 cm and 0.4 mm thick sections of selected  $\text{TaO}_2\text{F}$  hot-pressed samples. The CTE of hot-pressed  $\text{TaO}_2\text{F}$  was measured over 25–600 °C using a Perkin Elmer ThermoMechanical Analyzer (TMA) model TMA7 according to the ASTM E831-06 Standard Test Method for Linear Thermal Expansion of Solid Materials [3]. For CTE measurements, the  $\text{TaO}_2\text{F}$  samples were cut into 8

(10 mm × 3 mm × 4 mm) bars. Select samples were also heat-treated at 600 °C for 24 h in air prior to CTE measurements. No correction was made for the TMA machine thermal characteristics in the CTE data presented.

### 3. Results and discussion

#### 3.1. Consolidation of synthesized $\text{TaO}_2\text{F}$ powder via hot-pressing

The X-ray diffraction (XRD) pattern of the synthesized  $\text{TaO}_2\text{F}$  powder calcined at 300 °C is shown in Fig. 1, along with the overlay of JCPDS pattern for  $\text{TaO}_2\text{F}$  (cubic). The XRD pattern in Fig. 1 indicates a phase-pure cubic  $\text{TaO}_2\text{F}$  powder was formed after calcining at 300 °C.

The SEM images in Fig. 2 show the as-synthesized  $\text{TaO}_2\text{F}$  powders are highly agglomerated. Agglomerated powders are difficult to densify, and the resulting microstructures are non-uniform consisting of dense, large-grained and porous, fine-grained regions. Therefore, the as-synthesized  $\text{TaO}_2\text{F}$  powders were ball-milled for 4–24 h to break-up hard agglomerates, reduce the primary particle size, and achieve a narrower particle size distribution. The SEM image in Fig. 3 shows that ball-milling for 24 h reduced the  $\text{TaO}_2\text{F}$  particle size to less than 10 µm. However, the shapes of the  $\text{TaO}_2\text{F}$  particles are oblong with sharp edges, as opposed to spherical, which can inhibit densification during hot-pressing. XRD data for the milled powder showed that no reactions, phase changes, or impurities were incorporated during the milling process.

The stability of the  $\text{TaO}_2\text{F}$  as-synthesized powders in air and argon (Ar) at temperatures up to 1200 °C was investigated using thermal gravimetric analysis (TGA) and differential thermal analysis (DTA). Results indicated the stability of  $\text{TaO}_2\text{F}$  during use in air environments at atmospheric pressures

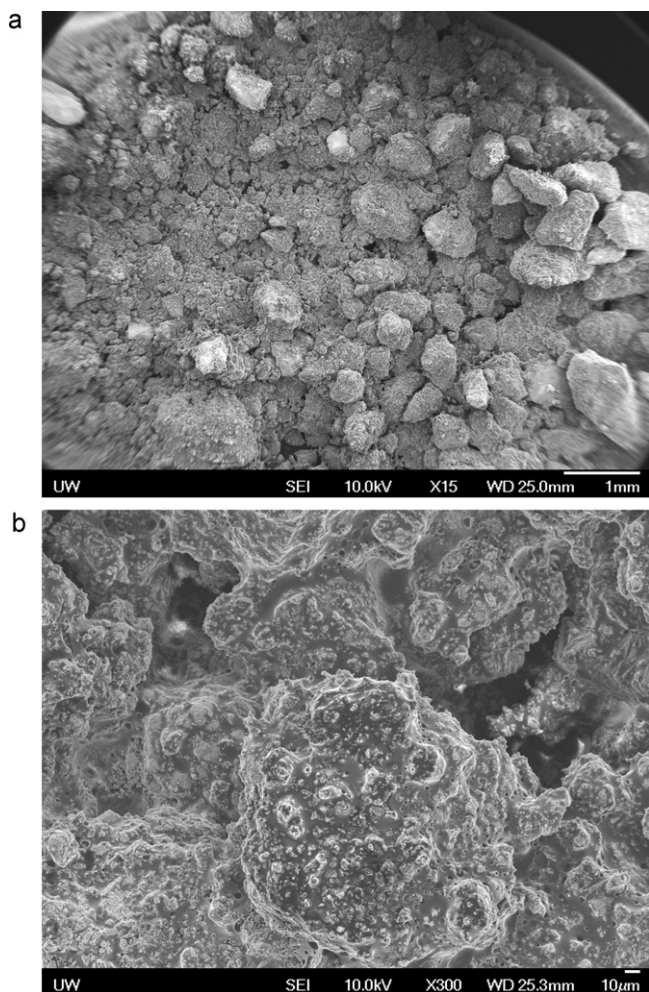


Fig. 2. SEM image of as-synthesized  $\text{TaO}_2\text{F}$  powder (before milling) at (a)  $\times 15$  and (b)  $\times 300$  magnification.

and indicated suitable processing environments for consolidation of  $\text{TaO}_2\text{F}$  via pressureless sintering or hot-pressing. TGA/DTA data for the ball-milled  $\text{TaO}_2\text{F}$  powder is given in Fig. 4. Identical results were obtained with the as-synthesized (agglomerated)  $\text{TaO}_2\text{F}$  powder.

The DTA and TGA results indicate that the  $\text{TaO}_2\text{F}$  powder is stable, or its decomposition is very slow, in both air and Ar at temperatures up to 750–800 °C. Weight loss of  $\text{TaO}_2\text{F}$  powder at approximately 800 °C was nearly 20% in both environments indicating it is no longer stable and may decompose at or above this temperature.

$\text{TaO}_2\text{F}$  powders could not be densified by hot pressing at 800 °C. Hot-pressing  $\text{TaO}_2\text{F}$  powders at temperatures below 800 °C in argon without a sintering aid resulted in porous and brittle compacts that fell apart after removal from the die. We then hot pressed  $\text{TaO}_2\text{F}$  powders at temperatures above the decomposition temperature of  $>800$  °C for up to 1 h in an attempt to densify  $\text{TaO}_2\text{F}$  without causing it to decompose. It was hoped that the kinetics of decomposition of  $\text{TaO}_2\text{F}$  were slow enough to allow densification without appreciable  $\text{TaO}_2\text{F}$  decomposition.

Thermochemical calculations using the HSC code [4] show that reactions between  $\text{TaO}_2\text{F}$  and carbon (C) become

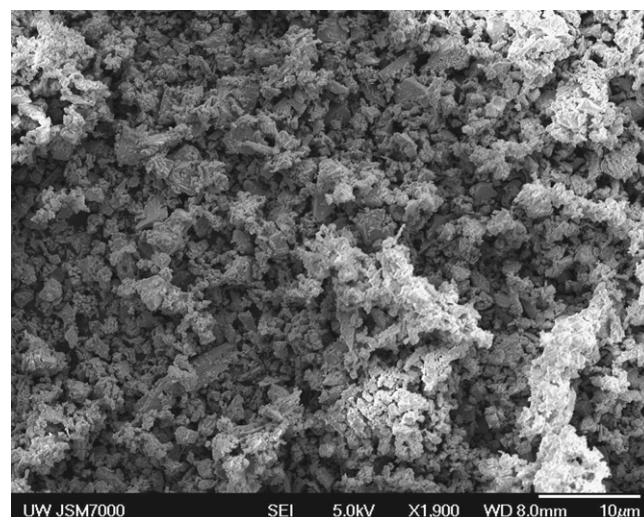


Fig. 3. SEM image of  $\text{TaO}_2\text{F}$  powder ball-milled for 24 h.

thermodynamically favorable at temperatures  $\geq 1200$  °C forming tantalum carbide (TaC); therefore, temperatures of  $\leq 1200$  °C, and preferably in the range of 900–1000 °C, were initially used for hot-pressing. We subsequently found that increasing the temperature beyond 1200 °C or increasing the holding time during hot-pressing at a relatively low applied pressure of 60 MPa caused a negative movement of the strain

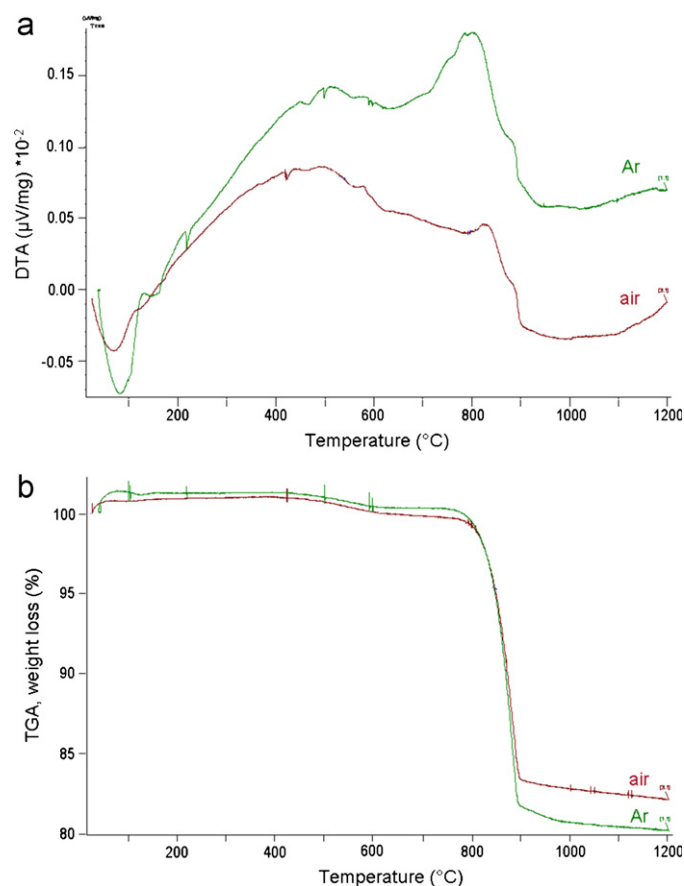


Fig. 4. (a) DTA and (b) TGA results for  $\text{TaO}_2\text{F}$  powder in air and argon (Ar) at temperatures up to 1200 °C.



Table 1

Density of hot-pressed TaO<sub>2</sub>F samples as a function of processing variables.

| TaO <sub>2</sub> F sample | Sintering aid | Temp (°C) | Pressure (MPa) | Hold time (min) | Density (g/cm <sup>3</sup> ) | Theoretical density <sup>a</sup> (%) |
|---------------------------|---------------|-----------|----------------|-----------------|------------------------------|--------------------------------------|
| 1                         | None          | 950       | 80             | 20              | 5.1                          | 78                                   |
| 2                         | None          | 1200      | 60             | 50              | 6.1                          | 94                                   |
| 3                         | None          | 1500      | 100            | 10              | 5.9                          | 91                                   |
| 4                         | 1.0 wt.% NaF  | 950       | 100            | 120             | 6.3                          | 97                                   |
| 5                         | 0.5 wt.% NaF  | 950       | 80             | 10              | 5.6                          | 85                                   |
| 6                         | 0.5 wt.% NaF  | 950       | 100            | 120             | 6.1                          | 93                                   |
| 7                         | 0.25 wt.% NaF | 1200      | 100            | 30              | 6.4                          | 99                                   |

<sup>a</sup> Theoretical density of TaO<sub>2</sub>F is calculated to be 6.517 g/cm<sup>3</sup> from the XRD lattice parameters.

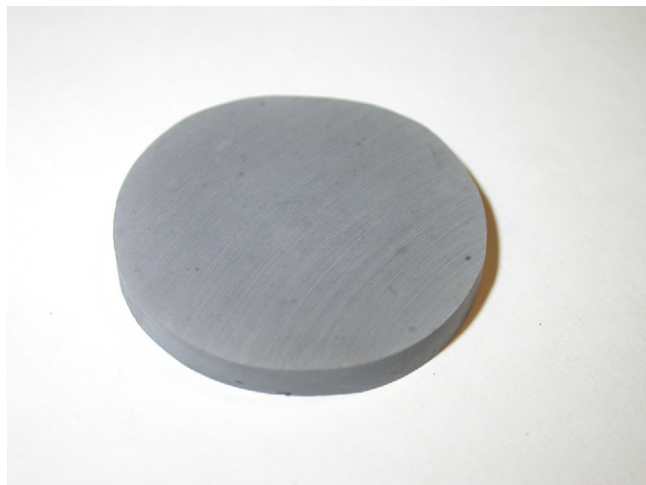
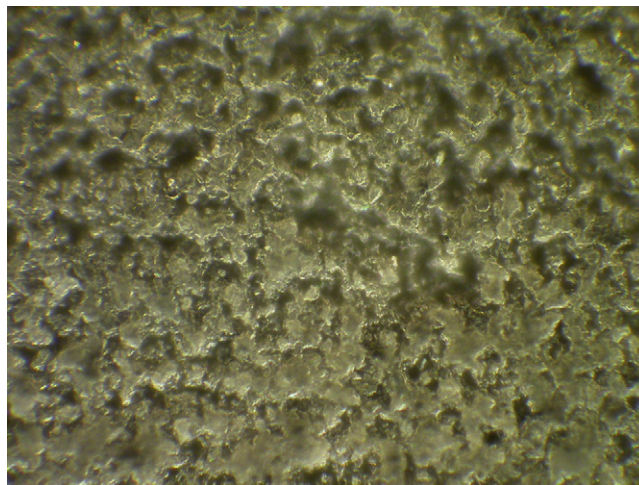
gage that monitors the compaction of the powder being pressed suggesting an increase in the volume of TaO<sub>2</sub>F sample. XRD data indicated that TaO<sub>2</sub>F samples hot-pressed at 1200 °C did not contain TaC; therefore, either the kinetics of the reaction between TaO<sub>2</sub>F and carbon are slow at this temperature and/or the concentration of TaC was very low (<0.1%) and could not be detected by XRD.

Reported phase transitions in TaO<sub>2</sub>F occur at 0.7 and 4.0 GPa [6], which are well above the pressures (46–100 MPa) employed for hot-pressing in this study. Therefore, we can rule out the phase transitions for observed volume increase during hot pressing. Structural characterization studies carried by Frevel and Rinn [5] show that TaO<sub>2</sub>F adopts a cubic ReO<sub>3</sub>-type structure that can also be compared to an undistorted ABX<sub>3</sub> perovskite with the A sites empty. In the ReO<sub>3</sub> structure, the framework MO<sub>6</sub> octahedral is rigid while the void spaces between them readily allow for considerable flexibility associated with the tilting of the MO<sub>6</sub> octahedra [6]. The ReO<sub>3</sub>-type structure is responsible for the near-zero thermal expansion of TaO<sub>2</sub>F and is also likely to be responsible for the unusual behavior of the TaO<sub>2</sub>F ceramic under compression during hot-pressing. Additional work is needed to gain a better understanding of the densification behavior of TaO<sub>2</sub>F and to determine the cause of its apparent volume expansion at high temperatures (≥1200 °C).

Densities of hot-pressed TaO<sub>2</sub>F compacts with and without sintering aid are given in Table 1 as a function of pressing

parameters. Notice that the TaO<sub>2</sub>F sample hot-pressed at 1500 °C at a higher applied pressure (100 MPa) has a lower density than the sample hot-pressed at 1200 °C and 60 MPa despite a higher temperature and greater applied pressure. TaO<sub>2</sub>F sample (sample 1 in Table 1) hot-pressed at 950 °C is shown in Fig. 5. Light optical microscope image of the polished cross-section of the sample 1 in Fig. 6 shows significant macroporosity in the microstructure.

All of the hot-pressed TaO<sub>2</sub>F samples in this study were grey in color; whereas, the starting TaO<sub>2</sub>F powder (as-synthesized or milled) was white. We attempted to gain some insight into densification of TaO<sub>2</sub>F by carrying out pressureless sintering experiments in air, vacuum, argon (Ar), and pure oxygen (O<sub>2</sub>) environments. At least we wanted to understand the color change from white to grey in TaO<sub>2</sub>F during hot-pressing since it is generally associated by impurity incorporation or stoichiometry change in the material. Pressureless sintering of TaO<sub>2</sub>F samples resulted in a near zero increase in density, i.e., no densification occurred, therefore, results from these experiments are not presented here. However, TaO<sub>2</sub>F samples pressureless sintered at 500–700 °C in vacuum or argon environments were grey or black in color. XRD showed that all samples were phase-pure TaO<sub>2</sub>F. This observation indicates that oxygen depletion may cause the color change in TaO<sub>2</sub>F from white to grey. Grey-colored samples may therefore be non-stoichiometric, or oxygen-deficient, TaO<sub>2-δ</sub>F. The samples pressureless sintered in air and in pure O<sub>2</sub> at the same

Fig. 5. TaO<sub>2</sub>F sample 1 hot-pressed at 950 °C and 80 MPa.Fig. 6. Cross-sectional view of microstructure of TaO<sub>2</sub>F sample 1 (×50).

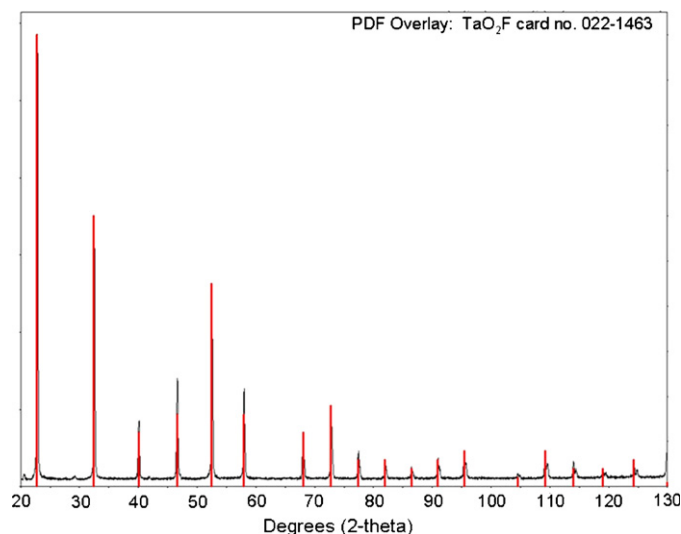


Fig. 7. XRD pattern for TaO<sub>2</sub>F sample 2 hot-pressed at 1200 °C and 60 MPa with TaO<sub>2</sub>F PDF overlay (No. 022-1463).

temperature, 700 °C were white. XRD showed the sample sintered in air was phase pure TaO<sub>2</sub>F while the sample sintered in pure O<sub>2</sub> contained TaO<sub>2</sub>F and smaller amounts of Ta<sub>2</sub>O<sub>5</sub>. It has been reported that upon heating in dry O<sub>2</sub> above 500 °C TaO<sub>2</sub>F decomposes into Ta<sub>2</sub>O<sub>5</sub> and TaF<sub>5</sub> [5], the latter of which is highly volatile and likely evaporates. Both Ta<sub>2</sub>O<sub>5</sub> and stoichiometric TaO<sub>2</sub>F are white in color, which is consistent with the white color of the samples.

The relatively high density (94% theoretical) of sample 2 in Table 1 indicates that TaO<sub>2</sub>F was somewhat densified under the pressing conditions. We determined that densification of TaO<sub>2</sub>F mostly occurred at temperatures in the range of 900–1000 °C by monitoring the ram movement using an LVDT gage. The XRD pattern for sample 2 is given in Fig. 7, which suggests that it is phase-pure TaO<sub>2</sub>F. Small shoulder peaks in the peaks at higher angles (>90°) were caused by the instrument radiation source and could be eliminated by reducing the slit size used to filter the incoming X-rays. The results demonstrated that hot-pressing TaO<sub>2</sub>F at high temperatures up to 1200 °C, above its decomposition temperature of 800 °C, did not cause it to decompose or react with the graphite liner.

We then investigated sintering aids to increase the density of polycrystalline TaO<sub>2</sub>F by hot-pressing. The selected sintering aid must be effective at very low concentrations (<0.5–1.0 wt.%) to preserve the characteristics of TaO<sub>2</sub>F including high IR transparency and a near zero CTE. The sintering aid must not form precipitates at the grain boundaries that would otherwise cause IR scattering. We considered fluorine salts, such as lithium fluoride (LiF), sodium fluoride (NaF), or magnesium fluoride (MgF<sub>2</sub>), as a sintering aid for TaO<sub>2</sub>F since they are known to promote sintering of ceramic materials. These fluorine salts are also IR transparent and therefore may also be used to produce a dense TaO<sub>2</sub>F with high IR transparency.

NaF was selected as a sintering aid since its melting temperatures of 993 °C is about the densification temperature of TaO<sub>2</sub>F (900–1000 °C). TaO<sub>2</sub>F powder with NaF was

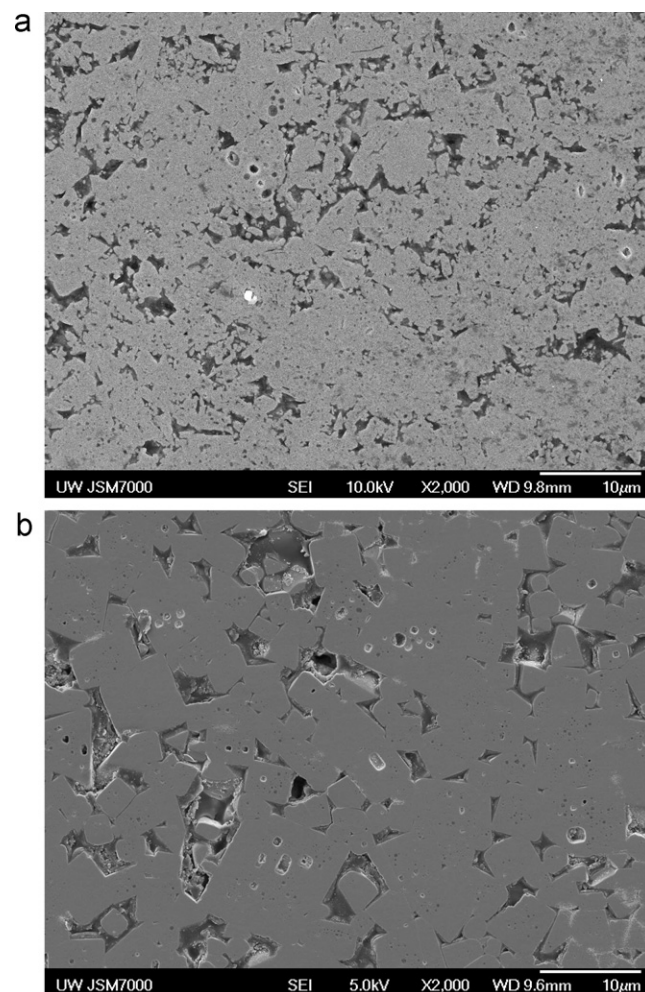


Fig. 8. SEM images of cross-sections of TaO<sub>2</sub>F hot-pressed at 950 °C and 80 MPa (a) sample 1, and (b) sample 5.

hot-pressed at temperatures of 950–1200 °C. Physical property data for hot-pressed TaO<sub>2</sub>F samples containing NaF are given in Table 1 along with the samples that were hot pressed without a sintering aid.

Comparing the physical property data for TaO<sub>2</sub>F samples 1 and 4 clearly show that addition of NaF to TaO<sub>2</sub>F promotes densification during hot-pressing. The highest density (99% theoretical) was achieved using a small amount of sintering aid (0.25 wt.% NaF) and hot-pressing at 1200 °C (TaO<sub>2</sub>F sample 7). All of the samples in Table 1 were processed in oxygen-deficient environments and were grey in color, indicating they may be slightly depleted of oxygen or a slightly non-stoichiometric TaO<sub>2-x</sub>F phase.

SEM was used to examine the effect of sintering aid (NaF) on the microstructure, e.g., grain size, porosity, and grain boundary structure of hot pressed TaO<sub>2</sub>F. SEM images of microstructures of sample 1 (without sintering aid) and sample 5 (with 0.5 wt.% NaF) are shown in Fig. 8. Samples 1 and 5 were both hot-pressed at 950 °C and 80 MPa (see Table 1); therefore, any differences in their microstructures and physical properties were caused by presence of NaF sintering aid. The SEM images in Fig. 8 show that addition of NaF promotes

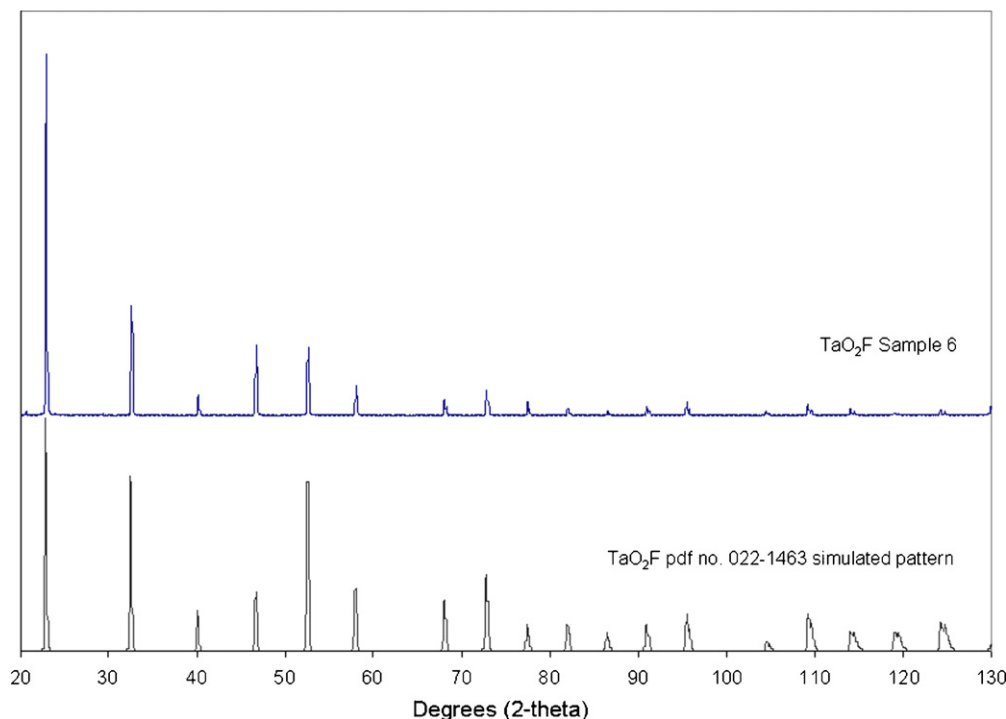


Fig. 9. XRD pattern for TaO<sub>2</sub>F sample 6 with 0.5% NaF hot-pressed at 950 °C.

densification of TaO<sub>2</sub>F evidenced by reduced porosity in sample 5 (Fig. 8b). However, it also causes grain growth. The grains in sample 5 (Fig. 8b) are much larger than those in sample 1 with no sintering aid (Fig. 8a). It is possible that a dissolution–precipitation mechanism, in which TaO<sub>2</sub>F dissolves in NaF and then precipitates out, causes densification and grain growth.

Sample 6 containing 0.5 wt.% NaF was analyzed by XRD to determine the presence of any second phase in the hot pressed TaO<sub>2</sub>F. The XRD pattern of sample 6 is shown in Fig. 9. The peaks in the XRD pattern in Fig. 9 match those in the JADE reference pattern for TaO<sub>2</sub>F (PDF No. 022-1463). However, the relative intensities of peaks at 47.6° and 52.5° in the XRD

pattern for sample 6 do not match those in reference pattern. Since the XRD pattern was acquired using a crushed powder sample, the different intensities of the peaks are not due to a preferred orientation and may be due to incorporation of Na or F into the TaO<sub>2</sub>F lattice during hot-pressing. NaF or new phases may have also formed in the sample at concentrations below the detection limits of XRD (less than ~0.1% volume). A TaO<sub>2</sub>F sample with 10 wt.% NaF was hot-pressed at 750 °C and analyzed using XRD to determine if NaF reacts with TaO<sub>2</sub>F and forms new phases under hot pressing conditions. The XRD pattern for hot-pressed TaO<sub>2</sub>F with 10% NaF shown in Fig. 10 contains many peaks in addition to those for TaO<sub>2</sub>F and NaF indicating that they reacted to form other compounds. Peak

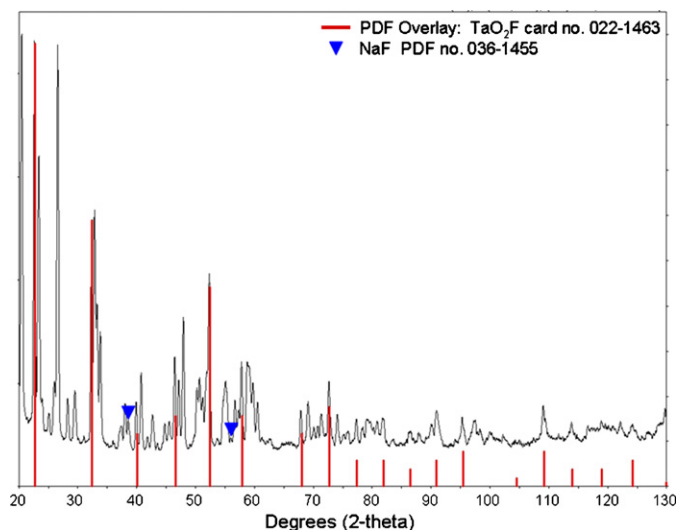


Fig. 10. XRD pattern for TaO<sub>2</sub>F with 10% NaF hot-pressed at 750 °C.

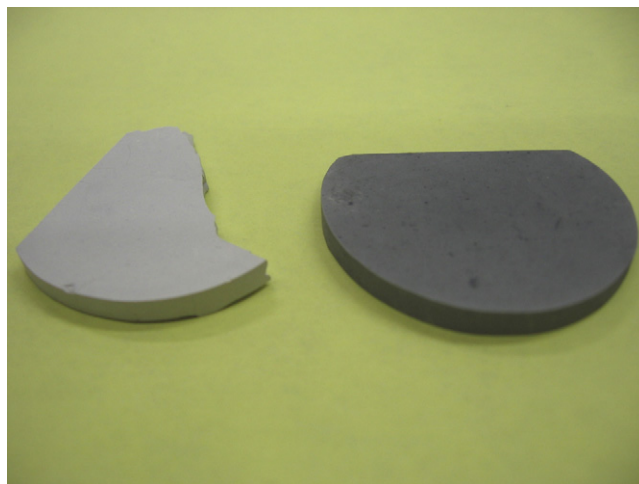


Fig. 11. Images TaO<sub>2</sub>F sample 1 before (right) and after (left) heat-treatment at 500 °C in air for 12 h showing a color change from grey to white.



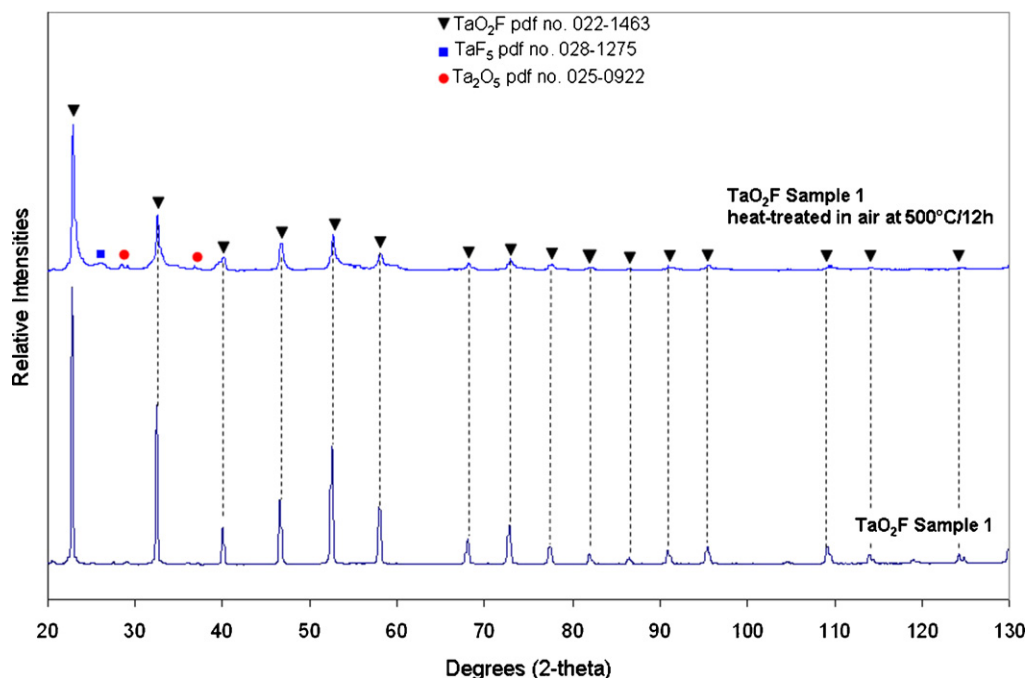


Fig. 12. XRD patterns for hot-pressed TaO<sub>2</sub>F Sample 1 before and after heat-treatment in air at 500 °C for 12 h.

matching indicated the presence of Na<sub>2</sub>Ta<sub>3</sub>O<sub>6</sub>F<sub>5</sub> (PDF No. 025-0871), and Ta (PDF No. 004-0788), and there were many other peaks that did correspond to any reference patterns in the JCPDS catalog and could not be identified. This experiment indicates that new compounds, such as Na<sub>2</sub>Ta<sub>3</sub>O<sub>6</sub>F<sub>5</sub>, will form in TaO<sub>2</sub>F samples containing NaF, but may be present in concentrations too low to detect using XRD. However, even trace amounts of other phases in TaO<sub>2</sub>F can affect its optical and IR transparencies.

### 3.2. Stability of consolidated TaO<sub>2</sub>F in air

It has been reported that TaO<sub>2</sub>F powders decompose upon heating in air at 500 °C (Frevel and Rinn [5]); however, Tao and Sleight [1] did not observe any chemical instability in their work up to 525 °C. Using DTA/TGA analysis we determined that TaO<sub>2</sub>F powder is stable for at least short periods of time (<10 min) in air up to 750–800 °C (see Fig. 4). Based on these results, we can predict that the densified polycrystalline TaO<sub>2</sub>F, which have lower surface areas than the starting powder, will be stable in air up to 750–800 °C for 10 min or longer. To determine the long term (h) stability of TaO<sub>2</sub>F in air, TaO<sub>2</sub>F sample 1 in Table 1 (78% dense) was subjected to heat-treatment in air at 500 °C for 12 h. This sample was initially dark grey in color indicating it was non-stoichiometric TaO<sub>2</sub>F and subsequently turned white after the heat-treatment in air as shown in the images in Fig. 11. XRD patterns for sample 1 before and after heat-treatment in air at 500 °C for 12 h are shown in Fig. 12.

The XRD pattern in Fig. 12 (bottom) shows that after 12 h at 500 °C in air, TaO<sub>2</sub>F begins to decompose into Ta<sub>2</sub>O<sub>5</sub> (PDF No. 025-0922) and TaOF<sub>3</sub> (calculated). Considering the long length of time of the heat-treatment, the amount of TaO<sub>2</sub>F decomposed was small based on the relative peak heights for Ta<sub>2</sub>O<sub>5</sub> and

TaOF<sub>3</sub> in the XRD pattern. It is also important to remember that since sample 1 was initially grey in color indicating it may be oxygen deficient (non-stoichiometric TaO<sub>2-δ</sub>F) and, typically, non-stoichiometric ceramics have faster diffusion rates than their pure stoichiometric counterparts since crystal defects such as oxygen vacancies and cation vacancies, etc., can contribute to the diffusion. In addition, sample 1 was highly porous (22% porosity), and has a higher exposed surface area and thus larger reaction cross-section than fully dense TaO<sub>2</sub>F making it more susceptible than densified TaO<sub>2</sub>F to decomposition at elevated temperatures in oxidative environments for extended periods of time. The results indicate that decomposition of fully dense and stoichiometric TaO<sub>2</sub>F is possible at 500 °C in air, but that the kinetics of its decomposition is relatively slow.

### 3.3. IR transmission measurements

The synthesized phase-pure TaO<sub>2</sub>F powder was analyzed by FT-IR spectroscopy to confirm that TaO<sub>2</sub>F does not have any inherent absorption bands in mid-IR region (3–5 μm). The IR spectrum for TaO<sub>2</sub>F using the KBr pellet method in Fig. 13 shows there are no inherent absorption bands in pure TaO<sub>2</sub>F from 2.5 μm to 6.3 μm.

IR transparencies of polished cross-sections (0.4–0.5 mm thickness) of hot-pressed TaO<sub>2</sub>F samples from Table 1 were negligible, i.e., not measurable. This was not surprising since the samples had 1% or more porosity and were dark grey in color indicating they were depleted of oxygen and non-stoichiometric.

IR scattering in TaO<sub>2</sub>F may be mitigated through material processing improvement, i.e., removal of pores and consolidation of stoichiometric TaO<sub>2</sub>F to full density (>99.9% dense) with no precipitates or impurities. However, TaO<sub>2</sub>F proved to

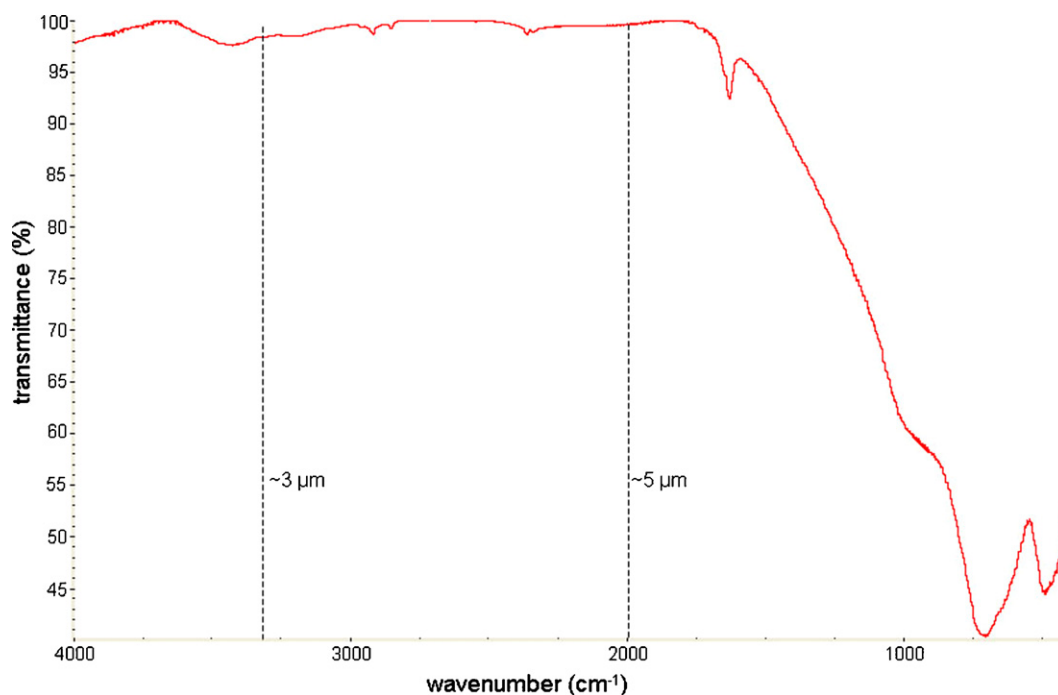


Fig. 13. IR spectrum for synthesized TaO<sub>2</sub>F powder acquired from KBr pellet method.

be difficult to consolidate to full density without altering its chemical properties, i.e., oxygen and/or stoichiometry. Further work is needed to understand the densification behavior of polycrystalline TaO<sub>2</sub>F.

### 3.4. CTE measurements

The CTE of hot pressed TaO<sub>2</sub>F with 0.5% NaF (sample 6 in Table 2) were measured over 25–600 °C. Half of the test samples were heat-treated at 600 °C for 24 h in air, turning their color from grey to white, before CTE measurements. This was carried out to investigate how changes in the oxygen content in TaO<sub>2</sub>F affect the CTE. Sample 7 in Table 1 was not used for these measurements despite its high theoretical density since it was darkest in color and subsequent heat-treatments in air failed to produce a white ceramic. Sample 4 was not used for these measurements despite its higher density due to its relatively high NaF content (1 wt.%).

CTE data for sample 6 are given in Fig. 14 and tabulated in Table 2. The data shows that the CTE of partially densified

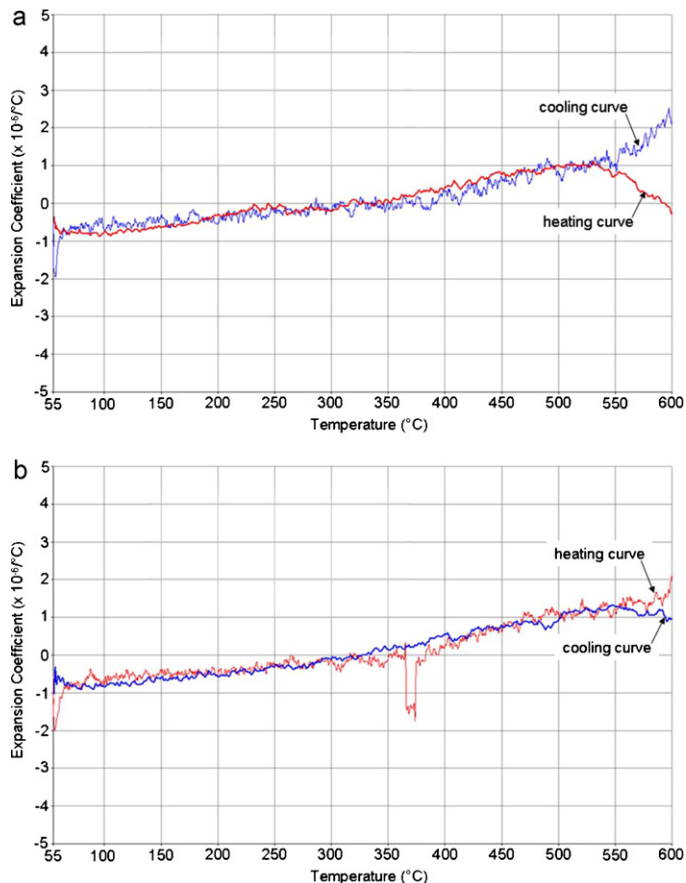


Fig. 14. CTE data up to 600 °C for (a) white TaO<sub>2</sub>F and (b) grey TaO<sub>2</sub>F.

Table 2

CTE of hot pressed TaO<sub>2</sub>F bars before (grey) and after (white) heat-treatment in air.

CTE over 25–600 °C ( $\times 10^{-6} \text{ }^{\circ}\text{C}^{-1}$ )  
Heating/cooling

| Grey                  | White (heat-treated in air) |
|-----------------------|-----------------------------|
| 0.14/0.12             | 0.14/0.09                   |
| 0.16/0.04             | 0.27/0.07                   |
| 0.12/0.01             | 0.12/0.07                   |
| 0.12/0.14             | 0.11/0.09                   |
| Avg = $0.11 \pm 0.05$ | Avg = $0.12 \pm 0.06$       |



(93% dense) polycrystalline TaO<sub>2</sub>F appears to be non-linear over the test temperatures. Hot pressed TaO<sub>2</sub>F contracts slightly from 25 °C to 300 °C, and then expands slightly from 350 °C to 600 °C.

The average CTE of grey and white TaO<sub>2</sub>F bars over 25–600 °C were  $0.11 \pm 0.05 \times 10^{-6} \text{ }^{\circ}\text{C}^{-1}$  and  $0.12 \pm 0.06 \times 10^{-6} \text{ }^{\circ}\text{C}^{-1}$ , respectively. The CTE of the hot pressed TaO<sub>2</sub>F (both white and grey) were somewhat less than that for pure, stoichiometric TaO<sub>2</sub>F powder over 25–500 °C ( $0.29 \times 10^{-6} \text{ }^{\circ}\text{C}^{-1}$ ) from Tao and Sleight [1]. Since the CTE of hot pressed TaO<sub>2</sub>F is extremely low, the thermal characteristics of the TMA machine may have influenced the CTE data in Table 2. The CTE of the TMA machine is expected to be slightly positive, which means the CTE values in Table 2 may be slightly overestimated. Nonetheless CTE data suggests that hot pressed, polycrystalline TaO<sub>2</sub>F has a near-zero thermal expansion, which suggests a high thermal shock resistance.

#### 4. Conclusions

Densification of TaO<sub>2</sub>F to >90% dense via hot-pressing at temperatures below 1200 °C could not be achieved without use of NaF sintering aids. Densities of 93–97% (percent theoretical density) were achieved by hot-pressing TaO<sub>2</sub>F with 0.5–1.0 wt.% NaF at 950 °C. The color of TaO<sub>2</sub>F powder changed from white to grey under hot-pressing conditions indicating that the hot-pressed material may be oxygen-deficient TaO<sub>2-δ</sub>F. Processing parameters to form a fully dense (>99.9%) stoichiometric (white) TaO<sub>2</sub>F still need to be determined.

DTA/TGA data for TaO<sub>2</sub>F powder indicates that TaO<sub>2</sub>F is stable for at least short periods of time (<10 min) in air at temperatures up to 700–800 °C. However, experiments carried out by heat-treating partially dense TaO<sub>2</sub>F samples for extended periods of time (h) indicate it can undergo a very slow decomposition at temperatures of  $\geq 500 \text{ }^{\circ}\text{C}$  in air.

Synthesized white TaO<sub>2</sub>F powder has no inherent absorption bands in the IR region of 3–5  $\mu\text{m}$ ; however, hot-pressed TaO<sub>2</sub>F

samples had near zero IR transparencies that were not measurable. The poor IR transparency of hot-pressed TaO<sub>2</sub>F was likely due to (i) changes in the TaO<sub>2</sub>F stoichiometry during hot-pressing, (ii) residual porosity, and/or (iii) presence of secondary phases.

The CTE of consolidated TaO<sub>2</sub>F is near-zero over 25–600 °C. Hot-pressed TaO<sub>2</sub>F has a CTE that is extremely low (near zero) regardless of its color, i.e., oxygen stoichiometry. Dense polycrystalline TaO<sub>2</sub>F may have a high thermal shock resistance due to its near-zero thermal expansion coefficient.

#### Acknowledgements

Program funding was provided by the Naval Air Warfare Center under the Small Business Innovative Research (SBIR) Program under Contract No. N68335-08-C-0300. The authors would like to thank Prof. Art Sleight and Dr. Dan Harris of NAWC, China Lake, CA, for helpful discussions, Dr. Brian Flinn for TGA analysis and CTE measurements, and Avery Sakshaug of Sienna Technologies, Inc. for conducting laboratory experiments.

#### References

- [1] J.Z. Tao, A.W. Sleight, Very low thermal expansion in TaO<sub>2</sub>F, *J. Solid State Chem.* 173 (2003) 45–48.
- [2] R. Apetz, M.P.B. van Bruggen, Transparent alumina: a light scattering model, *J. Am. Ceram. Soc.* 86 (2003) 480.
- [3] ASTM E831-06 Standard Test Method for Linear Thermal Expansion of Solid Materials.
- [4] HSC Chemistry<sup>®</sup> Version 5.0, Outokumpu Research Oy, Finland. ISBN 952-9507-08-9, 2002.
- [5] L.K. Frevel, H.W. Rinn, The crystal structure of NbO<sub>2</sub>F and TaO<sub>2</sub>F, *Acta Crystallogr.* 9 (1956) p626.
- [6] M. Cetinkol, A.P. Wilkinson, C. Lind, W.A. Bassett, C.-S. Zha, High-pressure powder diffraction study of TaO<sub>2</sub>F, *J. Phys. Chem. Solids* 68 (2007) 611–616.